

## Phonon and electron-phonon renormalization in Al-doped MgB<sub>2</sub>

G. Profeta and A. Continenza

*Istituto Nazionale di Fisica della Materia (INFM) and Dipartimento di Fisica, Università degli Studi di L'Aquila, I-67010 Coppito (L'Aquila), Italy*

S. Massidda

*Istituto Nazionale di Fisica della Materia (INFM) and Dipartimento di Fisica, Università degli Studi di Cagliari, 09124 Cagliari, Italy*  
(Received 17 July 2003; published 7 October 2003)

A detailed *ab initio* study of the electronic properties of the Al-doped MgB<sub>2</sub> compound is reported. The  $E_{2g}$  phonon frequency is calculated as a function of the Al content within linear-response theory. Our results show that a strong phonon frequency renormalization starts at 25% Al content, explaining the phonon frequency behavior as a function of Al doping reported by different experiments.

DOI: 10.1103/PhysRevB.68.144508

PACS number(s): 74.25.Jb, 74.62.Dh, 74.70.Ad, 74.70.Dd

Two years after the report of superconductivity in MgB<sub>2</sub>,<sup>1</sup> many properties of this compound have been investigated and understood in many respects. In particular, the mechanisms that lead to superconductivity are right now quite well established:<sup>2</sup> the strong electronic coupling with a particular phonon mode (the zone center  $E_{2g}$ ) and the number of holes at the Fermi level in the  $\sigma$  B bands have been demonstrated to lead to a transition temperature  $T_c$  as high as 39 K.<sup>2,3</sup> Unfortunately, the understanding of the mechanism did not help to further improve the superconducting properties of MgB<sub>2</sub>. Based on a possible increase of the hole density of states (within a rigid-band scheme), it was suggested—but never demonstrated—that hole doping could further increase  $T_c$ . From the experimental side, however, hole doping in MgB<sub>2</sub> remains a challenging goal to achieve: incorporation of proper dopants is very difficult due to structural changes and phase separations that turn out to suppress, rather than increase,  $T_c$ .

As a paradox, the first, and the only successful, alloying of the MgB<sub>2</sub> structure was achieved with the electron-dopant Al. Thanks to the very stable AlB<sub>2</sub> phase, Al substitution within the Mg network is possible at any concentration, and at 50% doping the formation of an ordered stable AlMgB<sub>4</sub> phase has been reported.<sup>4</sup> Many experiments as well as theoretical calculations appeared on Mg<sub>1-x</sub>Al<sub>x</sub>B<sub>2</sub> compounds, focused on understanding the mechanisms that lead to superconducting degradation. These alloys are in fact particularly interesting since they allow to monitor the structural, electronic, and superconducting properties as a continuous function of electron doping.

Mainly, the decrease of  $T_c$  upon Al addition has been explained in terms of changes in the Fermi-surface topology.<sup>5,6</sup> Lately, two related works<sup>4,7</sup> pointed out the renormalization of the  $E_{2g}$  phonon frequency in going from AlB<sub>2</sub> to MgB<sub>2</sub>. Both papers discuss the behavior of the  $E_{2g}$  phonon frequency as a function of increasing Al content and clearly show an anomaly in the curve at about 20%–25% Al concentration, where the phonon frequency is seen to increase abruptly.

The changes induced by doping to physical parameters, such as lattice constants ( $a$  and  $c$ ), carrier density, phonon frequency, and density of states at the Fermi level, are inti-

mately related to the superconducting phase transition. Therefore, the study of all these physical quantities in Mg<sub>1-x</sub>Al<sub>x</sub>B<sub>2</sub> represents a unique opportunity to study the interplay of all these parameters and to understand how they influence the critical temperature of MgB<sub>2</sub>. We can identify two different effects that jointly lead to a  $T_c$  reduction as  $x$  increases: (i) a positive pressure effect—due to the smaller Al ionic radius—and (ii) the increased number of electrons contributed by Al. Both effects are crucial. First-principles electronic structure calculations, in addition with density-functional perturbation theory, represent the only method available to properly take into account all these important ingredients and to study in detail electronic band structures, phonon frequencies, and electron-phonon coupling  $\lambda$ . We use the first-principles pseudopotential approach,<sup>8</sup> within the virtual-crystal (VC) approximation to account for the effect of disorder when substituting Al on the Mg sites. Norm-conserving pseudopotentials were used for all the elements considered, Mg  $p$  semicore states were not included in the valence, and their contribution to the exchange and correlation potential was accounted for by the nonlinear core corrections. All the intermediate phases at different Al content are obtained through linear interpolation from the calculated structural parameters of pure MgB<sub>2</sub> and AlB<sub>2</sub>. We verified that Vegard's law is generally fulfilled within 1%, comparing with fully optimized supercells at selected concentrations<sup>9</sup> and with optimized VC structures (as also found in Ref. 6). The calculations were carried out within the local-density approximation to the exchange-correlation potential. A  $20 \times 20 \times 15$   $k$ -point grid in the Brillouin zone, a Gaussian smearing 0.15 eV, and an energy cutoff of 38 Ry were found to give a satisfactory convergence for all the calculated quantities. The calculated structural parameters for MgB<sub>2</sub> (AlB<sub>2</sub>) are  $a=5.758$  a.u. and  $c/a=1.144$  ( $a=5.585$  a.u. and  $c/a=1.088$ ). The electron-phonon interaction strength is calculated according to<sup>10,11</sup>

$$\lambda = N_h^\sigma(E_F) \frac{\hbar^2}{2M_B \omega^2} \sum_j \left| \sum_a \varepsilon_a^j D_a \right|^2, \quad (1)$$

where  $D_a$  is the deformation potential of the  $\sigma$  bands at the  $\Gamma$  point per B atoms,  $j$  runs over the two degenerate  $E_{2g}$

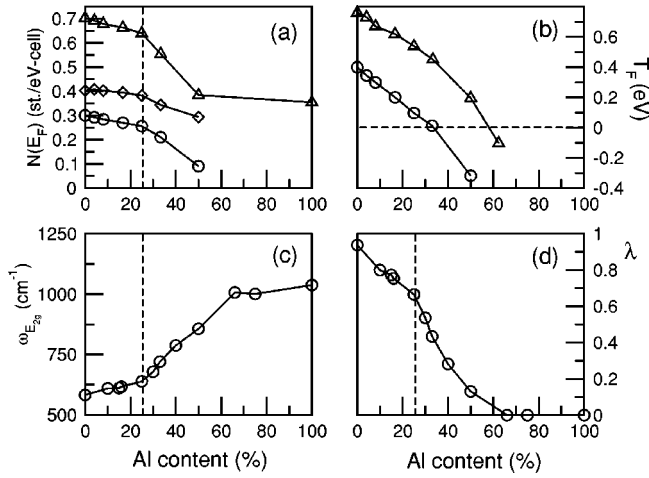


FIG. 1. (a) B  $\sigma$  (circles),  $\pi$  (diamonds), and total (triangles) density of states at the Fermi level. (b) Energy distance of the  $\sigma$  bands at  $\Gamma$  (circles) and at A (triangles). (c) Frequency of the  $E_{2g}(\mathbf{q}=0)$  phonon mode. (d) Electron-phonon coupling constant for the  $E_{2g}$  mode at the  $\Gamma$  point [ $\lambda_{E_{2g}}(\mathbf{q}=0)$ ]. All the quantities are plotted as a function of the Al content.

modes,  $a$  over the two moving B atoms,  $N_h^\sigma$  is the hole number per spin per cell in the  $\sigma$  bands at the Fermi level,  $\varepsilon_j^a$  represents the unitary displacement along the  $E_{2g}$  phonon eigenvectors for each B atom, and the frequency is expressed in terms of the corresponding energy.

Figure 1 summarizes our main results as a function of Al content. In panel (a) we report the behavior of the contribution of the B  $\sigma$  and  $\pi$  bands to the density of states at the Fermi level, as obtained from a spline fit of the *ab initio* bands. The value of  $N_\sigma$  at  $x=0$  is 0.3 states/eV cell and decreases as the Al concentration is increased. We note a monotonic decrease, with an abrupt change of slope occurring at about  $x=25\%$  (marked by a vertical dashed line). In panel (b), the energy difference between the Fermi level and the top of the  $\sigma$  bands at the  $\Gamma$  and A point (i.e., the hole Fermi temperature for perfectly two-dimensional bands) is plotted as a function of  $x$  and is in agreement with similar calculations.<sup>6</sup> The monotonic decreasing trend, related to the filling of the  $\sigma$  bands, is characterized by a change of slope occurring at about  $x=33\%$ : at this concentration the Fermi temperature goes to zero indicating the complete filling of the  $\sigma$  bands at the  $\Gamma$  point. At higher Al doping, the Fermi level touches the  $\sigma$  bands along the  $\Gamma$ -A line,<sup>5</sup> marking the transition from a pure two-dimensional (2D) Fermi surface to an overall three dimensional (3D) dispersion regime. Both quantities shown in Fig. 1 [panels (a) and (b)] describe how Al addition changes the electronic properties of  $\text{MgB}_2$ ; the presence of two different regimes as a function of  $x$  calls for a deeper investigation of the dynamical properties.

As stated in the beginning, the existence of low-energy phonon frequencies, strongly coupled to  $\sigma$  electrons at  $E_F$ , is the fundamental property that makes the  $\text{MgB}_2$  compound so special in comparison with all the other diborides. The experimental determination of the phonon spectrum of the alloyed compounds revealed interesting features; a corresponding complete theoretical estimate, however, is still

lacking. The only theoretical results available are those for  $x=50\%$  phase,<sup>7,9</sup> where an interesting structural phase transition to a supercell-like structure, with a doubling of the  $c$  lattice parameter, has been reported. The main result of these studies is that the filling of the  $\sigma$  bands and the contraction of the lattice constants increase the phonon frequency of the mixed compound. We calculated the behavior of the  $E_{2g}$  phonon frequency as a function of  $x$ : our results are shown in Fig. 1, panel (c). We see that in going from the superconducting ( $\text{MgB}_2$ ,  $x=0\%$ ) to the nonsuperconducting phase ( $\text{AlB}_2$ ,  $x=100\%$ ), the phonon frequency jumps from  $575 \text{ cm}^{-1}$  to  $1000 \text{ cm}^{-1}$ , with rather abrupt changes at  $x \approx 25\%$  and  $x \approx 66\%$ . Moreover, three different regimes can be easily identified: the first one ( $0\% < x < 25\%$ ) is characterized by a slow variation of the phonon frequency, the second one ( $25\% < x < 66\%$ ) reveals a rapid increase of the frequency, while the last one ( $x > 66\%$ ) shows a saturation behavior to the  $\text{AlB}_2$  value. This result evidentiates that phonon renormalization does not vary smoothly with electron doping; in addition, the first discontinuity in the phonon curve occurs at about 25%, slightly less than 33%, where the transition from the 2D to the 3D Fermi surface is predicted. The only direct link between band-structure features and anomalies in the phonon frequency behavior can be traced back to the  $\pi$  hole pockets around the  $M$  point that completely disappear at about 25% doping. The second discontinuity occurs at about  $x=66\%$ , a doping level actually larger than the value (about 60%) which fills out completely the  $\sigma$  bands.

Although observed experimentally, this phonon renormalization at about  $x=25\%$  was never clearly pointed out, due to difficulties in the assignment of the various components and to phase inhomogeneities. In Ref. 7, however, the phonon frequency renormalization is shown to be nonlinear and characterized by a pronounced jump at  $x \approx 20\%$ . In addition, the results of Ref. 4 indicate that the onset of the phonon changes occurs at about  $x=25\%$ .

Due to the virtual-crystal approach used in our calculations, we do not consider structural phase transitions or phase separations at any Al content. In fact, we find that the  $a$  and  $c$  lattice parameters decrease roughly linearly as the Al content is increased, without any of the anomalies observed in experiment.<sup>12,13</sup> Nevertheless, the main features of the  $E_{2g}$  phonon frequency behavior as a functions of Al content appear clearly and well reproduce the experimental findings: this shows that they are related to band-structure effects, rather than to bare structural features.

It could be interesting to study the behavior as a function of Al doping of the other modes. However, within virtual-crystal approximation it is not obvious to assign a reasonable value to the mass of the virtual atom; nevertheless, modes such as the  $B_{1g}$  mode and the  $E_{2g}$  previously discussed, involving the out-of-plane motion of B atoms alone, could be predicted. The behavior of such a mode as a function of Al content is reported in Fig. 2.

The mode does not show any anomaly: the curve decreases smoothly moving from pure  $\text{MgB}_2$  to  $\text{AlB}_2$ , taking values at the end points in good agreement with previous calculations and experiments.<sup>14</sup> Interestingly, the  $B_{1g}$  mode

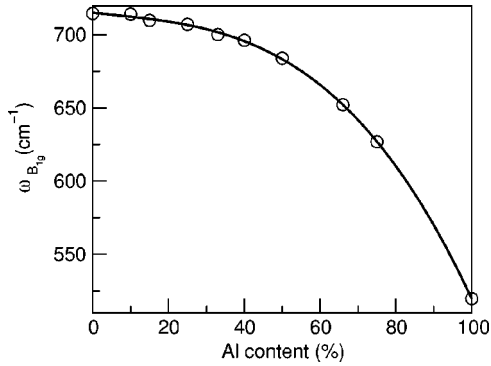


FIG. 2. Frequency of the  $B_{1g}(\mathbf{q}=0)$  phonon mode as a function of the Al content. The solid line shown is a spline fit of the data as a guide to the eye.

follows the opposite trend with respect to the  $E_{2g}$  mode, becoming softer as the Al content is increased. The different behavior of these phonon modes stresses the peculiarity of the coupling between  $\sigma$  electrons and the  $E_{2g}$  mode.

Let us now discuss the effect of Al doping on the electron-phonon coupling. As discussed by several authors,<sup>2,3,15</sup> the phonon mode most relevant to superconductivity in  $\text{MgB}_2$  is the  $E_{2g}$  mode; therefore, a good approximation to the electron-phonon coupling strength can be inferred using the zone-center mode only.<sup>3,11</sup> A more rigorous treatment of such a quantity requires summation over all phonon modes and the entire Brillouin zone;<sup>2</sup> however, this is beyond the goal of the present paper.

Panel (d) of Fig. 1 shows the plot of  $\lambda$  as a function of  $x$ . As expected, the electron-phonon coupling constant decreases as the Al content is increased; however, we remark that the deformation potential at the  $\Gamma$  point<sup>3</sup> remains almost constant ( $\approx 13$  eV/Å) with doping, in agreement with the results previously found in pure  $\text{MgB}_2$  and  $\text{AlB}_2$ .<sup>9,16</sup>

The calculation of  $\lambda(x)$  and of  $\omega_{E_{2g}}(x)$  allows to estimate  $T_c$ , and, more importantly, shows how they concur to  $T_c$  degradation. We can obtain an estimate of  $T_c(x)$  through the McMillan formula, using the calculated quantities and assuming as usual  $\mu^* = 0.1$ :  $T_c(x) = \omega_{E_{2g}}(x) / 1.2 \exp[-1.04(1 + \lambda(x)) / [\lambda(x)(1 - 0.62\mu^*) - \mu^*]]$ .

Several experimental studies focussed on the effects of Al addition in  $\text{MgB}_2$ , and in particular, reported the variation of the transition temperature as a function of  $x$ . Due to the approximations discussed above, we are not looking for a quantitative agreement: we therefore normalize our results to the  $T_c$  obtained for pure  $\text{MgB}_2$  in order to compare the predicted trend with available experiments.

In Fig. 3 [panel (d)] our results are shown, in comparison with the experiments (normalized at their respective  $x=0\%$  value) as given in Refs. 4,7, and 13 [panel (a), (b), and (c) respectively]. The agreement between the theoretical predictions and the various experimental data is rather good for  $x$  up to 30%, although the theoretical values show a more rapid  $T_c$  lowering as  $x$  increases. At larger  $x$  concentrations different experiments give different results, probably related to differences in sample preparation. Clearly, the contribution

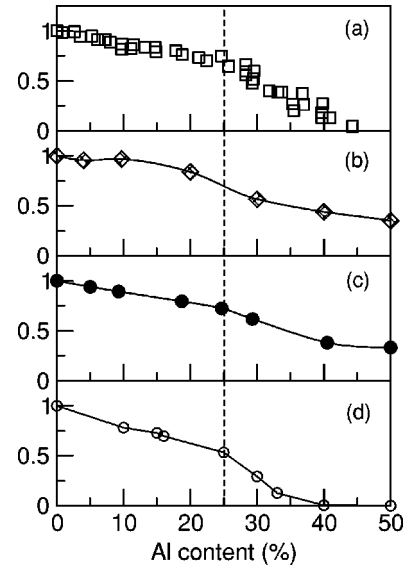


FIG. 3. Experimental  $T_c$  of  $\text{Mg}_{1-x}\text{Al}_x\text{B}_2$  samples as a function of  $x$  taken from Refs. 4,7 and 13 (panel (a), (b), and (c), respectively). The temperatures are normalized to the  $x=0$  value. Panel (d) calculated transition temperature as a function of Al content.

of  $\pi$  bands, neglected in our approach, should be included and could somehow change the  $T_c$  behavior.

It is interesting to stress that all the experiments are characterized by a change in the slope at about  $x=25\%$  (dashed vertical line in Fig. 3). This discontinuity is well reproduced by our calculation that shows the same feature. As discussed previously, the origin of this anomaly is related to changes in both the  $E_{2g}$  phonon frequency and the hole density of states at the Fermi level.

In conclusion, we report the first calculation of zone-center frequencies phonons, electron-phonon coupling constant, and  $T_c$  as a function of Al doping in  $\text{MgB}_2$ . Our results agree well with the details of the experimental results, showing how the  $E_{2g}$  phonon frequency and the electron-phonon coupling change in going from  $\text{AlB}_2$  to the superconducting material. We correctly reproduce the anomaly in the phonon curve at  $x=25\%$  found by experiments and show that it correlates with a similar behavior in the  $\sigma$  hole density of states. In addition, we found that the onset of the sharp decrease in  $\lambda$  is concomitant with a hardening of the  $E_{2g}$  mode.

Finally, it should be stressed that Al doping brings the system into a highly nonadiabatic regime, where conventional electron-phonon coupling theory is expected to fail.<sup>17,18</sup> Although the conventional approach is able to explain the main features of superconductivity in  $\text{MgB}_2$ ,<sup>3</sup> our calculations cannot quantify the importance of the effects beyond the Migdal approach.

This work was partially supported by Istituto Nazionale Fisica della Materia (INFN) through project PRA-UMBRA and “Iniziativa Trasversale Calcolo Parallelo,” and by the Italian Consiglio Nazionale delle Ricerche (CNR) through “Progetto 5% Applicazioni della superconduttività ad alta  $T_c$ .”

- <sup>1</sup>J. Nagamatsu, N. Nakagawa, T. Muranaka, Y. Zenitani, and J. Akimitsu, *Nature (London)* **410**, 61 (2001).
- <sup>2</sup>H.J. Chol, D. Roundy, H. Sun, M.L. Choen, and S.G. Louie, *Nature (London)* **418**, 758 (2002).
- <sup>3</sup>J. An and W. Pickett, *Phys. Rev. Lett.* **86**, 4366 (2001).
- <sup>4</sup>P. Postorino, A. Congeduti, P. Dore, A. Nucara, A. Bianconi, D.D. Castro, S.D. Negri, and A. Saccone, *Phys. Rev. B* **65**, 020507 (2001).
- <sup>5</sup>A. Bianconi, S. Agrestini, D. Di Castro, G. Campi, G. Zangari, N.L. Saini, A. Saccone, S. De Negri, M. Giovannini, G. Profeta, A. Continenza, G. Satta, S. Massidda, A. Cassetta, A. Pifferi, and M. Colapietro, *Phys. Rev. B* **65**, 174515 (2002).
- <sup>6</sup>O. de la Peña, A. Aguayo, and R. de Coss, *Phys. Rev. B* **66**, 012511 (2002).
- <sup>7</sup>B. Renker, K.B. Bohnen, R. Heid, D. Ernst, H. Schober, M. Koza, P. Adelman, P. Schweiss, and T. Wolf, *Phys. Rev. Lett.* **88**, 067001 (2002).
- <sup>8</sup>S. Baroni, A.D. Corso, S. de Gironcoli, and P. Giannozzi, URL: [www.pwscf.org](http://www.pwscf.org)
- <sup>9</sup>G. Profeta, A. Continenza, F. Bernardini, G. Satta, and S. Massidda, *Int. J. Mod. Phys. B* **16**, 1563 (2002).
- <sup>10</sup>F.S. Kahn and P.B. Allen, *Phys. Rev. B* **29**, 3341 (1984).
- <sup>11</sup>G. Profeta, A. Continenza, F. Bernardini, and S. Massidda, *Phys. Rev. B* **65**, 054502 (2002).
- <sup>12</sup>J.S. Slusky, N. Rogado, K.A. Regan, M.A. Hayward, P. Khalifah, T. He, K. Inumaru, S.M. Loureiro, M.K. Haas, H.W. Zandbergen, and R.J. Cava, *Nature (London)* **410**, 343 (2001).
- <sup>13</sup>J.Q. Li, L. Li, F.M. Liu, C. Dong, J.Y. Xiang, and Z.X. Zhao, *Phys. Rev. B* **65**, 132505 (2001).
- <sup>14</sup>K.B. Bohnen, R. Heid, and B. Renker, *Phys. Rev. Lett.* **86**, 5771 (2001).
- <sup>15</sup>T. Yildirim, O. Gülseren, J.W. Lynn, C.M. Brown, T.J. Udovic, Q. Huang, N. Rogado, K.A. Regan, M.A. Hayward, J.S. Slusky, T. He, M.K. Haas, P. Khalifah, K. Inumaru, and R.J. Cava, *Phys. Rev. Lett.* **87**, 037001 (2001).
- <sup>16</sup>L. Boeri, G. Bachelet, E. Cappelluti, and L. Pietronero, *Phys. Rev. B* **65**, 214501 (2002).
- <sup>17</sup>J.M. An, S.Y. Savrasov, H. Rosner, and W.E. Pickett, *Phys. Rev. B* **66**, 220502 (2002).
- <sup>18</sup>E. Cappelluti, S. Ciuchi, C. Grimaldi, L. Pietronero, and S. Strässler, *Phys. Rev. Lett.* **88**, 117003 (2002).